Check for updates

ChemSystemsChem

ChemSystemsChem
Chemistry Europe
European Chemical Societies Publishing

RESEARCH ARTICLE OPEN ACCESS

Substituent-Guided Routing in Chemical Reaction Networks

Yeonsoo Lim[1] | Gyunam Park[1,2,3] | Minho Lee[1,2,3] | Gyeonghun Lee[1] | Jonghwa Han[1,2,3] | Yukyeong Lee[1] | Jaeyoung Sung[1,2,3] | Sunbum Kwon[1]

[1]Department of Chemistry, Chung-Ang University, Seoul, Republic of Korea | [2]Creative Research Initiative Center for Chemical Dynamics in Living Cells, Chung-Ang University, Seoul, Republic of Korea | [3]Global Science Research Center for Systems Chemistry, Chung-Ang University, Seoul, Republic of Korea

Correspondence: Jaeyoung Sung (jaeyoung@cau.ac.kr) | Sunbum Kwon (skwon@cau.ac.kr)

Received: 7 February 2026 | **Revised:** 17 September 2026 | **Accepted:** 24 September 2026

Keywords: chemical reaction network | metabolism | out-of-equilibrium systems | reaction kinetics | substituent effect

ABSTRACT

Metabolism is a complex chemical reaction network (CRN) that distributes reaction flux across multiple pathways, and mimicking such routing is of central interest in the design of synthetic out-of-equilibrium systems. Here, we investigate a chemically driven transient oligoesterification network in which subtle structural modifications of 4-hydroxybenzoic acid monomers give rise to markedly different routing behaviors. Strongly electron-withdrawing substituents positioned *ortho* to the phenolic hydroxy group act as molecular traffic directors by modulating its nucleophilicity and thereby selectively enabling or suppressing specific reaction channels. This substituent-guided pathway selection directly links molecular structure to network routing and provides a programmable strategy for wiring synthetic CRNs in ways reminiscent of biological metabolic organization. These findings demonstrate how chemical modification can reconfigure network connectivity and advance the rational design of complex synthetic CRNs.

1 | Introduction

Biological hallmarks such as metabolism, self-replication, compartmentalization, information storage and transfer, and evolution emerge from the coordinated operation of chemical reaction networks (CRNs) that underpin each of these processes [1–11]. Among them, metabolism offers a particularly vivid illustration of how living systems regulate chemical flux by selectively engaging different domains of a CRN in response to fluctuations in nutrient availability, pH, temperature, or stress [12–15]. A canonical example is the *lac* operon, which allows enteric bacteria to gate the lactose-catabolism module of their metabolic network when the energetically favored carbon source, glucose, is depleted [16]. Beyond such regulatory switches, the global architecture of metabolic networks allows organisms to extract energy from diverse nutrient classes, including carbohydrates, proteins, and lipids. These distinct metabolic sectors ultimately converge on common molecular intermediates such as acetyl-CoA, providing a unified route to ATP production [17]. Crucially, metabolic networks themselves are not static but evolve through rewiring, mutation, and selection [18–20]. Throughout this process, core CRNs are preserved, while variations arise that reshape flux distributions and reaction connectivity. Such network-level flexibility reinforces functional stability and allows organisms to persist under environmental and evolutionary pressures.

This evolution-guided, context-dependent regulation of biological CRNs provides a strong conceptual basis for the design

Yeonsoo Lim, Gyunam Park, Minho Lee, and Gyeonghun Lee contributed equally to this work.

This is an open access article under the terms of the Creative Commons Attribution License, which permits use, distribution and reproduction in any medium, provided the original work is properly cited.
© 2026 The Author(s). *ChemSystemsChem* published by Wiley-VCH GmbH

of synthetic networks. Incorporating evolutionary concepts into synthetic network design may allow artificial CRNs to develop new functions and adjust to changing conditions in ways reminiscent of living systems [21–25]. These synthetic systems are powered by chemical fuels, light, electrical energy, or mechanical inputs and can exhibit transient supramolecular self-assembly, self-replication, sustained chemical oscillations, and other non-equilibrium behaviors [26–44]. By converting energy inputs into temporally regulated chemical responses, such networks have enabled applications ranging from time-controlled drug delivery and adaptive materials to chemical reservoir computing [45, 46].

In synthetic systems, the behavior of a CRN can be readily modulated through mild chemical modification of its components or input concentrations [47–50]. Such interventions make it possible to activate specific network nodes, redirect reaction fluxes, or even bypass kinetically favorable steps, thereby activating pathways that would otherwise remain inaccessible. These strategies highlight our ability to design and fine-tune synthetic CRNs that, albeit relatively simple, echo the adaptive flexibility of biological networks. This conceptual framework motivated us to investigate how subtle molecular variations influence the operation of chemically driven, out-of-equilibrium systems.

We recently reported a chemically driven oligoesterification system in which 4-hydroxybenzoic acid derivatives undergo transient covalent assembly in aqueous solution [51]. The system operates far from equilibrium through activation by EDC (1-ethyl-3-(3-dimethylaminopropyl)carbodiimide), which drives repeated carboxylic acid activation and condensation. Although the underlying mechanism is based on well-established nucleophilic acyl substitution, the resulting reaction network proved unexpectedly complex and highly dynamic. Kinetic analysis indicated the involvement of short-lived intermediates and revealed a densely interconnected network topology, including a parasitic pathway in which one oligomer is consumed through reactions with other network species.

In that study, we compared two monomeric building blocks, 3-bromo-4-hydroxy-5-nitrobenzoic acid and 4-hydroxy-3-nitrobenzoic acid (Figure 1). Both contain a strongly electron-withdrawing nitro substituent *ortho* to the phenolic hydroxy group, which attenuates phenolic nucleophilicity while enhancing the leaving-group ability of the corresponding phenoxide. Introduction of an additional bromo substituent further reduced phenolic nucleophilicity, shifting the balance toward carboxylate-mediated pathways. This substituent-dependent redistribution of reactivity reshaped the reaction flux and the dynamic behavior of the CRN, demonstrating the sensitivity of network operation to relatively subtle electronic and steric variations.

2 | CRN of the Dinitro Monomer

Here, we continue to investigate how molecular features of reactants govern network structure, node selection, and reaction dynamics. For this purpose, we prepared two monomers—4-hydroxy-3,5-dinitrobenzoic acid (**A**) and 4-hydroxy-3-nitro-5-(trifluoromethyl)benzoic acid (**B**)—each bearing an additional nitro or trifluoromethyl substituent, respectively, at the position

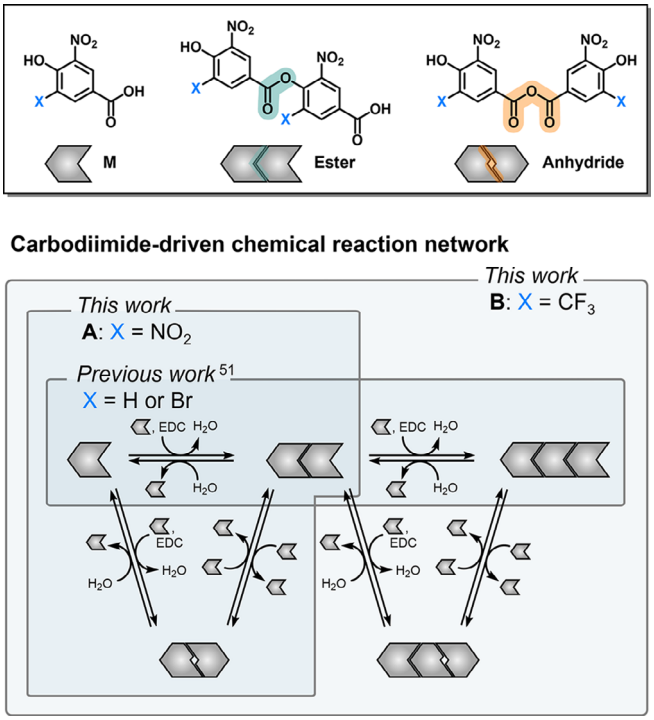


FIGURE 1 | Key observable species involved in the EDC-driven oligoesterification network of 4-hydroxybenzoic acid derivatives.

ortho to the hydroxy group (Figure 1). These nitro and trifluoromethyl groups are both bulkier and more strongly electron-withdrawing than the previously examined bromo substituent. First, we carried out the EDC-driven oligomerization of **A** in a 1:1 (*v*/*v*) mixture of acetonitrile and pyridine buffer (pH 5.5, 0.5 M) and monitored the reaction progress by ^{1}H NMR spectroscopy [52–56]. Upon addition of EDC, two new sets of signals appeared and were unambiguously assigned to the diester (**A_2-est**) and anhydride (**A_2-anh**) (Figures 2a and S2–S4). Aside from these dimeric products, no additional transient species were detected throughout the reaction. Consistent with this observation, the decrease in monomer concentration precisely matched the total amount of monomer incorporated into the dimers (2 × [**A_2-est**] + 2 × [**A_2-anh**]), indicating that longer oligomers are not formed under these conditions. Although formation of **A_2-est** proceeded slightly faster than that of **A_2-anh**, both species displayed nearly identical growth–decay profiles. This kinetic similarity suggests that the nucleophilicity of the hydroxy group is strongly attenuated by the two *ortho*-nitro substituents, allowing the carboxylate to compete effectively as a nucleophile.

Based on these experimental results, we constructed a kinetic model centered on a simplified reaction network, CRN **1** (Figure 2b and Table S2). In this CRN, EDC activates the carboxylic acid to form the *O*-acylisourea intermediate (**A-oai**, k_1), which is rapidly converted to the corresponding acyl pyridinium species (**A-ap**). Because no *N*-acylurea byproduct—an indicator of *O*-acylisourea rearrangement—was detected, the **A-oai** → **A-ap** conversion was assumed to be fast and was therefore omitted from kinetic fitting [55]. The **A-ap** intermediate then undergoes nucleophilic attack either by the hydroxy group or by the carboxylic acid of **A** to afford **A_2-est** (k_3) and **A_2-anh** (k_4), respectively. Formation of both dimeric species was treated as

25704206, 2026, 6, Downloaded from https://chemistry-europe.onlinelibrary.wiley.com/doi/10.1002/syst.70059 by Chung-Ang University, Wiley Online Library on [20/11/2026]. See the Terms and Conditions (https://onlinelibrary.wiley.com/terms-and-conditions) on Wiley Online Library for rules of use; OA articles are governed by the applicable Creative Commons License

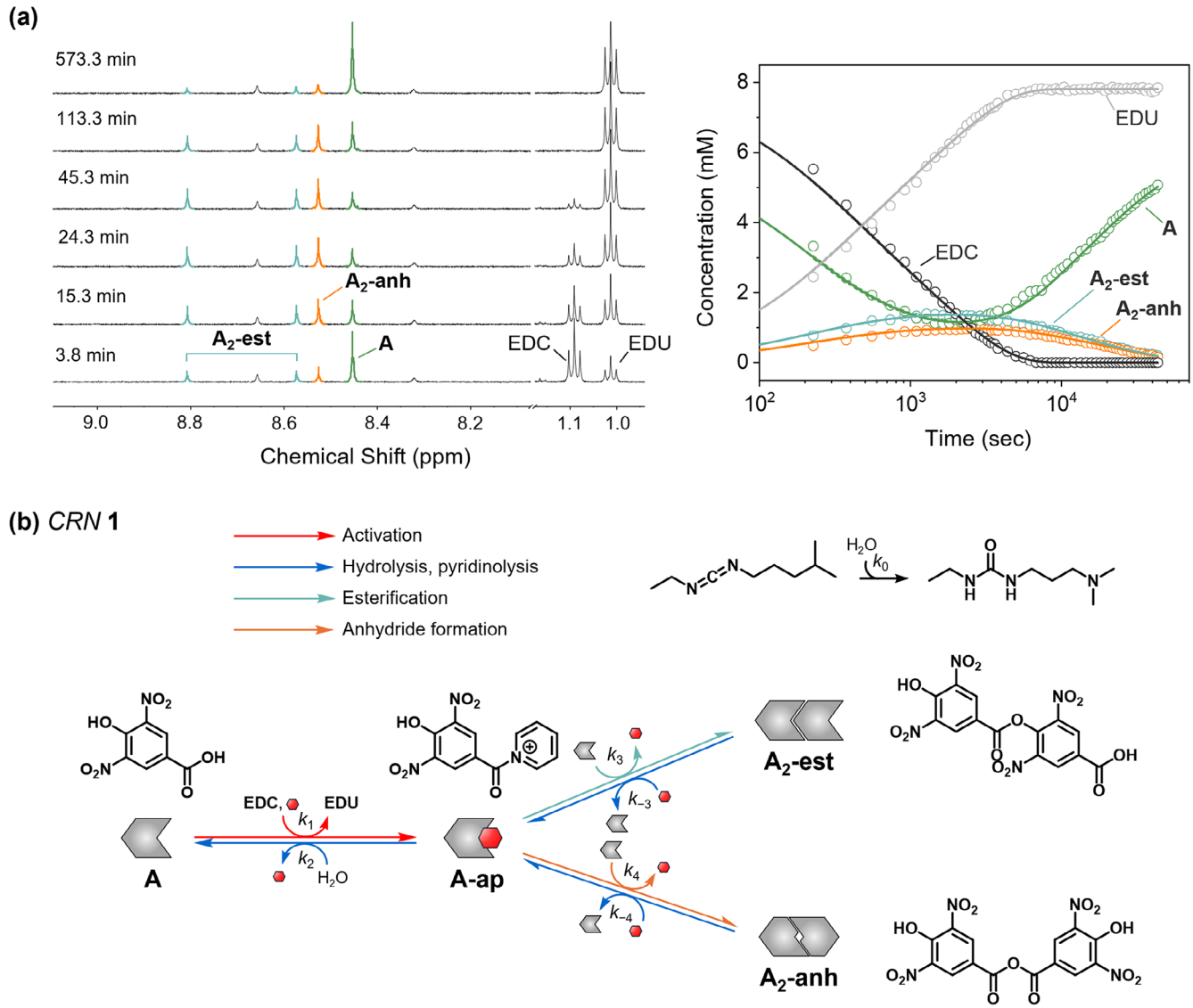


FIGURE 2 | (a) ^{1}H NMR monitoring of carbodiimide-driven transient oligoesterification of **A** (circles), recorded at 600 MHz in a 1:1 (*v*/*v*) mixture of pyridine/pyridinium D_2O buffer (pD 5.5, 0.5 M pyridine-d_5, 0.1 M NaCl, 80 mM DMA) and deuterated CD_3CN, and fits to the kinetic model for CRN **1** (solid lines). (b) Proposed chemical reaction network (CRN **1**).

reversible, with pyridinolysis of **A_2-est** and **A_2-anh** regenerating **A-ap** through k_{-3} and k_{-4}, respectively. The regenerated **A-ap** subsequently undergoes hydrolysis to **A** through the deactivation pathway k_2. In contrast, direct hydrolysis of **A_2-est** or **A_2-anh** was excluded because it was substantially slower than the corresponding pyridinolysis-mediated pathways under the kinetic conditions (Figures S5 and S6). Direct transacylation between the two dimers was likewise excluded, since incubation of either dimer in the absence of pyridine did not yield a measurable amount of the other.

Our kinetic model provides a quantitative explanation of the concentration–time profiles of all experimentally monitored species in the reaction network. To reduce parameter redundancy associated with the unobservable **A-ap** intermediate, a steady-state approximation was applied, such that k_2, k_3, and k_4 enter the model through the ratios $\alpha\,(=k_2/k_3)$ and $\beta\,(=k_2/k_4)$. Global fitting of the kinetic model to four independent datasets afforded five fit parameters (k_1, k_{-3}, k_{-4}, α, and β) and reproduced the growth and decay profiles of both dimeric species (Figure S7). The fitted parameters were consistent with comparable formation rates for **A_2-est** and **A_2-anh**, with a modest preference for **A_2-est** formation ($k_3/k_4 = \beta/\alpha = 1.45$, Table S3). Their fitted pyridinolysis rate constants were also similar ($k_{-3}/k_{-4} = 1.23$, Table S3). Pairwise heat maps of the regression error function revealed appreciable negative correlations between k_{-3} and α and between k_{-4} and β (Figure S8) [56–58]. The remaining parameter pairs showed no comparably strong interdependence, although several broad response surfaces indicated only moderate parameter constraints. Accordingly, the fitted values should be interpreted qualitatively rather than as precisely and independently determined kinetic parameters. Within this limitation, the analysis is consistent with comparable partitioning of **A-ap** into **A_2-est** and **A_2-anh** and with broadly similar pyridinolysis kinetics for the two dimers. This qualitative similarity is chemically reasonable: in **A_2-est**, the *ortho*-nitro substituents enhance the leaving-group ability of

25704206, 2026, 6, Downloaded from https://chemistry-europe.onlinelibrary.wiley.com/doi/10.1002/syst.70059 by Chung-Ang University, Wiley Online Library on [20/11/2026]. See the Terms and Conditions (https://onlinelibrary.wiley.com/terms-and-conditions) on Wiley Online Library for rules of use; OA articles are governed by the applicable Creative Commons License

the phenoxide through a strong mesomeric effect, whereas in **A_2-anh**, the *meta*-nitro groups stabilize the carboxylate through inductive withdrawal.

Notably, the triester **A_3-est** was not detected at any point, even within a regime where EDC, **A**, **A_2-est**, and **A_2-anh** coexist, conditions under which its formation would in principle be expected. Several plausible pathways can be envisaged for **A_3-est** generation, including reactions (1)–(3) below.

$$\begin{aligned} \mathbf{A} + \text{EDC} + \text{pyr} &\rightarrow \mathbf{A-ap} + \text{EDU} \\ \mathbf{A-ap} + \mathbf{A_2-est} &\rightarrow \mathbf{A_3-est} + \text{pyridine} \end{aligned} \tag{1}$$

$$\begin{aligned} \mathbf{A_2-est} + \text{EDC} + \text{pyr} &\rightarrow \mathbf{A_2-ap} + \text{EDU} \\ \mathbf{A_2-ap} + \mathbf{A} &\rightarrow \mathbf{A_3-est} + \text{pyridine} \end{aligned} \tag{2}$$

$$\mathbf{A_2-anh} + \mathbf{A_2-est} \rightarrow \mathbf{A_3-est} + \mathbf{A} \tag{3}$$

The absence of detectable **A_3-est** suggests that its formation is kinetically disfavored and/or that any **A_3-est** formed decays too rapidly to accumulate measurably. Consistent with the possibility that an **A_3** species is formed only transiently under strongly driven conditions, a trimeric species was indeed detected when a large excess of EDC (10 equiv.) was employed (Figures S9 and S10). This high-fuel condition was excluded from the kinetic analysis, however, because it resulted in uncontrolled precipitation. Accordingly, neglecting the formation of oligomers beyond the dimeric species introduced no inconsistencies in the kinetic analysis. Overall, these findings suggest that the set of reactive nodes accessible within CRN **1** is highly constrained, limiting the network's ability to engage in higher-order oligomerization or interconversion pathways.

3 | CRN of the CF_3 Monomer

Next, we investigated the transient oligomerization of **B** under conditions analogous to those used for **A**. Following the addition of EDC, four new sets of signals emerged in the ^{1}H NMR spectrum and were assigned to the diester (**B_2-est**), anhydride (**B_2-anh**), triester (**B_3-est**), and ester–anhydride heterotrimer (**B_3-het**) (Figures 3 and S11–S15). An ester–anhydride heterotrimer had been implicated but not directly observed in our earlier bromo-substituted system [51]. Here, **B_3-het** was directly detected, although it was short-lived and difficult to isolate in pure form. The **B** system exhibited several key features similar to those previously observed for the bromo-substituted system. First, **B_2-est** was markedly more persistent than **B_3-est**, with only 32% decaying over eight days of incubation. By contrast, **B_3-est** disappeared within approximately three hours. Second, after complete consumption of EDC—when further carbodiimide activation had ceased—the concentration of **B** did not recover concomitantly with the decay of **B_3-est** and **B_2-anh**. This observation cannot be explained by a simple model involving only EDC-driven chain growth followed by hydrolytic degradation. Instead, it points to the operation of scrambling pathways in which **B** is consumed through reactions with **B_3-est** and **B_2-anh**. These oligomeric species therefore act as reactive network nodes that undergo transacylation and redistribute material predominantly toward **B_2-est**. Collectively, these results demonstrate that the **B** system accesses a substantially more interconnected reaction network than the dimer-dominated **A** system.

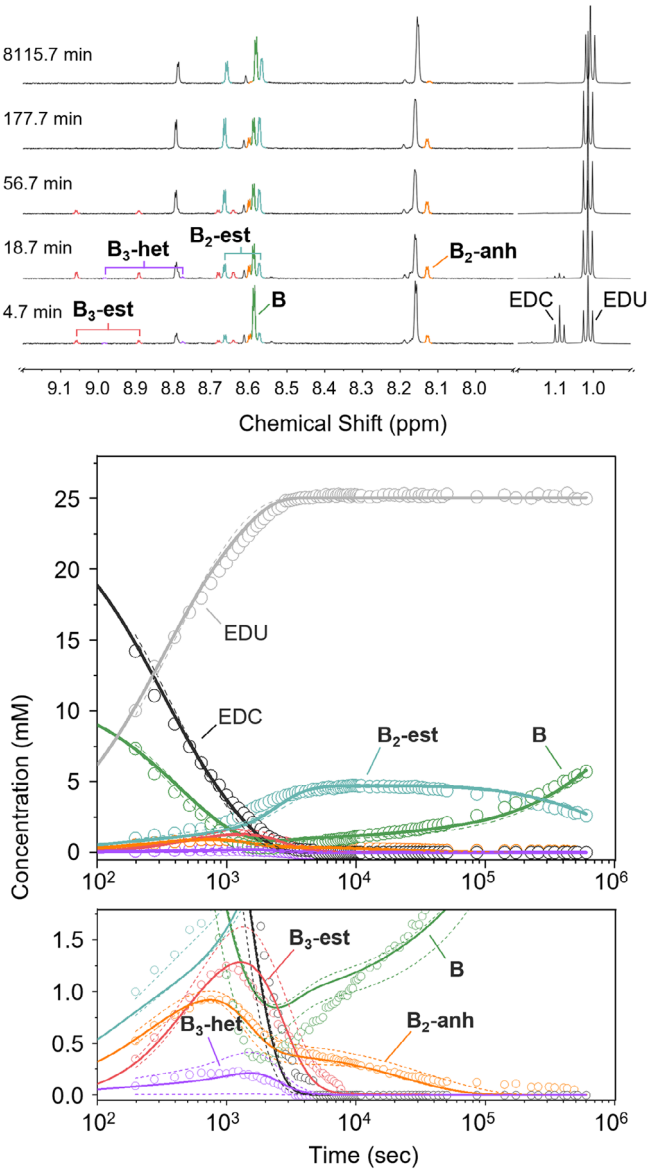


FIGURE 3 | ^{1}H NMR monitoring of carbodiimide-driven transient oligoesterification of **B** (circles), recorded at 600 MHz in a 1:1 (*v*/*v*) mixture of pyridine/pyridinium D_2O buffer (pD 5.5, 0.5 M pyridine-d_5, 0.1 M NaCl, 80 mM DMA) and deuterated CD_3CN, and fits to the kinetic model for CRN **2** (solid lines). The signals in the aliphatic region (0.9–1.2 ppm) are scaled down by a factor of 4 for clarity. The areas between the dashed lines indicate 95% confidence intervals for the fits.

We then constructed a kinetic model based on the plausible reaction network CRN **2** (Figure 4) to account for the dynamics of the **B** system. The model was adapted primarily from that previously developed for the bromo-substituted system and expanded to incorporate the experimentally observed **B_2-anh** and **B_3-het**, together with their associated formation, cleavage, and transacylation pathways. The ester–anhydride heterotetramer **B_4-het** was additionally included as a short-lived intermediate connecting

25704206, 2026, 6, Downloaded from https://chemistry-europe.onlinelibrary.wiley.com/doi/10.1002/syst.70059 by Chung-Ang University, Wiley Online Library on [20/11/2026]. See the Terms and Conditions (https://onlinelibrary.wiley.com/terms-and-conditions) on Wiley Online Library for rules of use; OA articles are governed by the applicable Creative Commons License

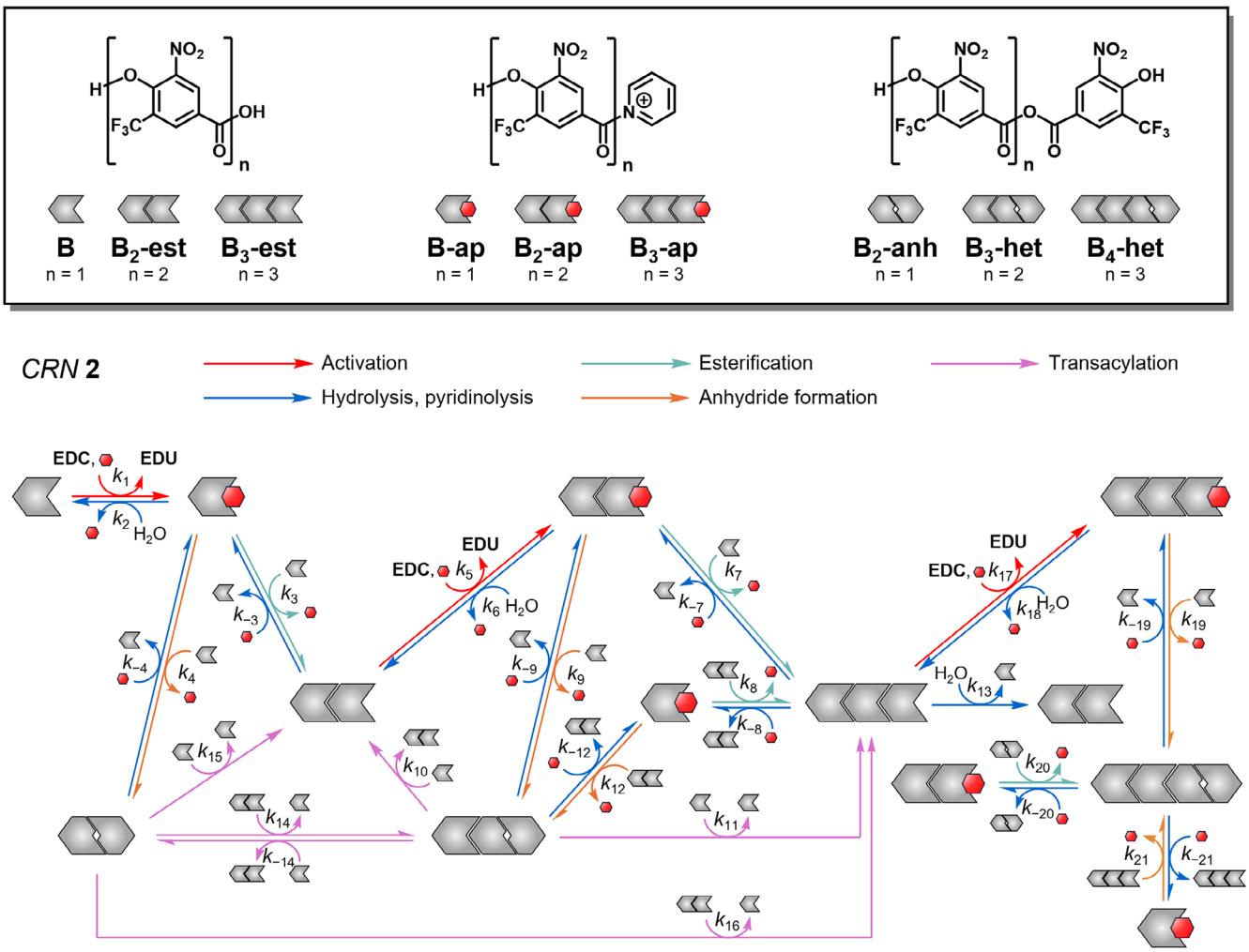


FIGURE 4 | Proposed chemical reaction network (CRN **2**).

several reaction pathways. Since its detailed connectivity and ester–anhydride linkage pattern were not independently determined, **B_4-het** was treated as an effective kinetic species rather than as a structurally assigned intermediate. Its inclusion provided a **B**-independent route to **B_2-anh** through pyridinolysis and allowed the model to reproduce the characteristic decay pattern of **B_2-anh** (see Section S3.3). In total, CRN **2** comprises 31 elementary reactions, excluding background EDC hydration. To reduce parameter redundancy associated with the unobservable acylpyridinium intermediates, steady-state approximations were applied to **B-ap**, **B_2-ap**, and **B_3-ap**, such that the corresponding branching reactions enter the model through ratios of rate constants. With the independently measured background EDC hydration rate constant k_0 held fixed, global fitting of four experimental datasets afforded 28 effective fit parameters and reproduced the time-dependent evolution of the experimentally monitored species reasonably well (Figure S18 and Table S5).

Given the size of CRN **2** and the likely interdependence among some of its fitted parameters, modest numerical differences between individual parameter values were not interpreted quantitatively. Instead, the model was used to identify pathway-level features required to account for the observed redistribution of material. Within this framework, **B_3-est** does not behave simply as a terminal product of oligomer growth but serves as a precursor to **B_3-het** and thereby participates in downstream scrambling reactions. Analysis of the calculated reaction fluxes identified the uncatalyzed reaction of **B_3-het** with **B** to form two molecules of **B_2-est** (k_{10}) as a major pathway for redistributing higher-order oligomeric species into the dimer pool. Since **B_3-est** feeds into **B_3-het** formation, this pathway links the depletion of **B_3-est**-derived higher-order species to the continued consumption of **B** after fuel exhaustion. A related scrambling pathway was previously proposed for the bromo-substituted system [51]. Collectively, these results show that higher-order intermediates, including species that do not accumulate to experimentally detectable concentrations, can function as active network nodes that redirect material through transacylation and scrambling rather than through simple hydrolytic degradation.

The broader implications of these observations are noteworthy. The **A** system collapses into a relatively simple network dominated by reversible dimer formation. By contrast, the **B** system accesses a substantially more interconnected topology comprising diester, triester, anhydride, and ester–anhydride heterotrimer nodes. Scrambling pathways involving a kinetically inferred heterotetrameric intermediate further redistribute material after fuel exhaustion. This contrast can be attributed largely

25704206, 2026, 6, Downloaded from https://chemistry-europe.onlinelibrary.wiley.com/doi/10.1002/syst.70059 by Chung-Ang University, Wiley Online Library on [20/11/2026]. See the Terms and Conditions (https://onlinelibrary.wiley.com/terms-and-conditions) on Wiley Online Library for rules of use; OA articles are governed by the applicable Creative Commons License

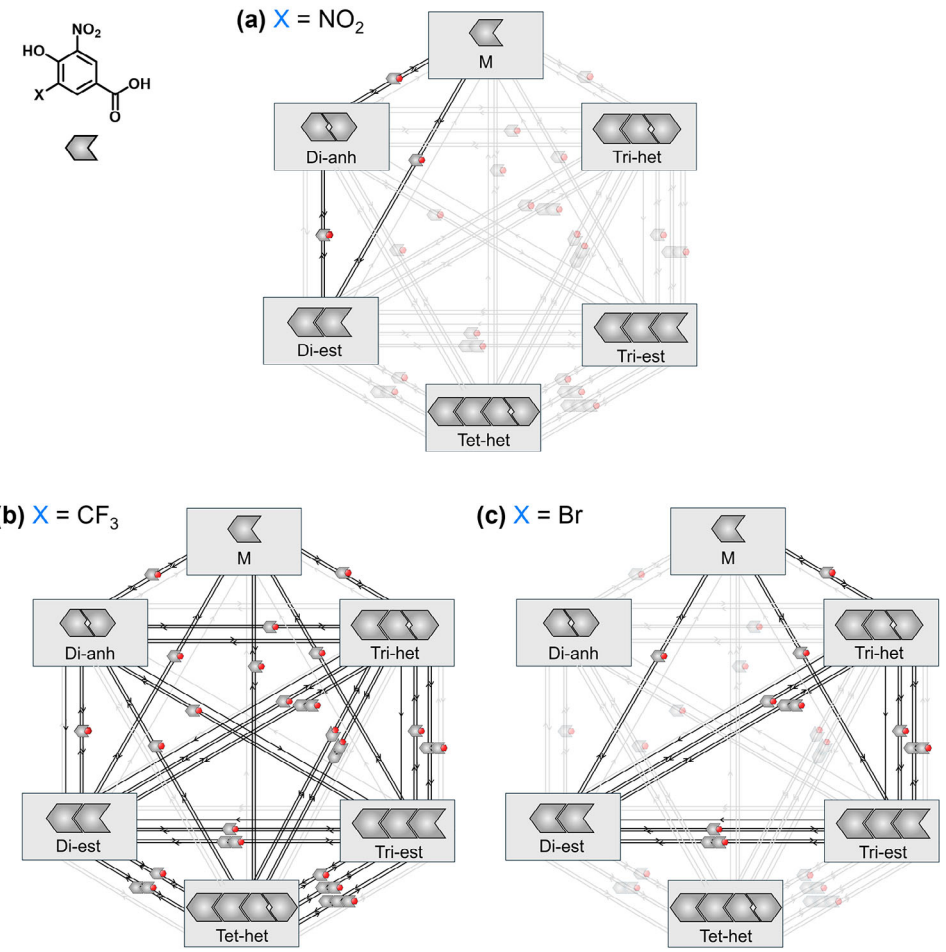


FIGURE 5 | The six-node network representations for the (a) nitro-, (b) trifluoromethyl-, and (c) bromo-substituted systems. Black lines denote key pathways required for fitting, while gray lines represent non-essential routes. Panel (c) was generated from a previously published dataset [51].

to the weaker electron-withdrawing effect of CF_3 relative to NO_2, despite the greater steric demand of CF_3, as reflected in their Hammett constants (σ_p = +0.54 and +0.78, respectively) and A values (2.1 and 1.1, respectively) [59–64]. Consistent with this interpretation, DFT calculations showed that **B** has a higher-lying monomer HOMO than **A** (−9.10 vs. −9.24 eV), supporting greater retention of phenolic nucleophilicity (Figure S29 and Table S6). This electronic balance facilitates successive *O*-acylation to form **B_2-est** and **B_3-est** while still permitting competitive anhydride formation. The persistence of **B_2-anh** further demonstrates that substituents regulate not only which network nodes are accessible but also their lifetimes. Collectively, these results illustrate how subtle structural modifications act as molecular selectors that reconfigure both the connectivity and dynamics of synthetic CRNs.

4 | Substituent-Guided Network Topology

Based on the kinetic analyses of the different systems, we constructed a comprehensive CRN framework to map activated reaction pathways and visualize their time-dependent dynamics. Six chemically distinct species classes—monomer, diester, anhydride, triester, ester–anhydride heterotrimer, and asymmetric ester–anhydride heterotetramer—were placed at the vertices of a hexagon as network nodes (Figure 5). Interconversions among these components are depicted as distinct routes, proceeding either through the corresponding acylpyridinium intermediates or via direct pathways. The minimal set of reaction pathways necessary to describe the experimentally observed dynamics is shown in black, whereas theoretically possible but non-essential routes are indicated in light gray. The **A** system exhibits a compact three-node topology dominated by exchange through the **A-ap** intermediate (Figure 5a and Movie S1). The presence of two strongly electron-withdrawing nitro substituents effectively suppresses further chain growth beyond the dimer, yielding a highly constrained CRN with markedly simple dynamics. In contrast, the kinetic representation of the **B** system incorporates all six nodes of the framework (Figure 5b and Movie S2). The weaker electron-withdrawing character of CF_3 preserves sufficient phenolic nucleophilicity for *O*-acylation despite its greater steric demand. Consequently, **B** participates in substantial flux through both ester and anhydride channels, and the ester–anhydride heterooligomers appear as active, albeit short-lived, intermediates. This expanded topology produces the richest and most interconnected dynamic behavior among the systems examined. Finally, the previously reported bromo-substituted system adopts an intermediate four-node topology (Figure 5c and Movie S3), in which monomer, diester, triester, and ester–anhydride heterotrimer remain dynamically

25704206, 2026, 6, Downloaded from https://chemistry-europe.onlinelibrary.wiley.com/doi/10.1002/syst.70059 by Chung-Ang University, Wiley Online Library on [20/11/2026]. See the Terms and Conditions (https://onlinelibrary.wiley.com/terms-and-conditions) on Wiley Online Library for rules of use; OA articles are governed by the applicable Creative Commons License

connected through reversible acylation and scrambling reactions, whereas the discrete anhydride node remains largely inaccessible [51].

The six-node network representations capture only a subset of the reaction pathways accessible under the specific experimental conditions used in this study. Modifying experimental conditions can dramatically expand the network. For example, increasing the EDC loading leads to the experimental appearance of additional higher oligomers, including multiple tetrameric, pentameric, and hexameric species, thereby extending the experimentally accessible network beyond the minimal six-node representation (Figures S19–S23). In principle, continued oligomer growth would generate a combinatorially large—and practically infinite—set of possible reaction pathways, far beyond what can be captured in a simplified schematic presentation [65, 66]. Furthermore, the current representation does not account for phase transitions, such as precipitation caused by the low solubility of oligomers, which can effectively remove species from the tractable portion of the network. Thus, while these diagrams offer a useful conceptual snapshot of the dominant nodes under defined conditions, they should not be interpreted as exhaustive maps of all chemically possible pathways.

Our results show that substituent effects can function as molecular wiring instructions, determining which portions of a CRN become activated under chemically driven, out-of-equilibrium conditions. By tuning the balance among hydroxy-group nucleophilicity, leaving-group ability, steric accessibility, and oligomer stability, substituents reshape the connectivity of EDC-driven CRNs, dictating whether a network accesses a highly interconnected, multipathway topology or collapses into a minimally connected one. Although the present study examines only a limited set of substituents, the observed trends suggest several preliminary design principles. Excessively strong electron withdrawal can suppress successive phenolic *O*-acylation and thereby limit chain elongation, whereas more moderate withdrawal can preserve esterification pathways and enable access to higher-order oligomers. Steric demand around the reactive groups may further bias otherwise competing transacylation pathways, while the stability and solubility of the resulting oligomers determine which network nodes remain dynamically accessible. Substituent selection should therefore be guided by a balanced consideration of electronic, steric, and physicochemical properties rather than by electron-withdrawing strength alone.

Future molecular designs could combine substituents with complementary roles on a single scaffold, with one group tuning nucleophilicity and another modulating steric environment, product stability, or solubility, thereby enabling more sophisticated control over node accessibility and lifetime. Building on our previously reported mixed-monomer system [51], mixtures of differently substituted building blocks could introduce selective homo- and hetero-oligomerization pathways whose relative fluxes depend on monomer composition and sequence, fuel loading, and the other chemical inputs. Such architectures may support tunable or logic-gated routing, in which distinct combinations of molecular and energetic cues selectively activate different regions of the network. More broadly, this progression from single-substituent control to multicomponent and multi-input systems may provide a route toward programmable synthetic CRNs that more closely emulate the context-dependent organization of biological metabolism [67, 68].

Acknowledgments

This work was supported by the National Research Foundation of Korea (NRF) grants (RS-2025-23323695 and RS-2024-00411134). We thank Prof. Hartley at Miami University for sharing the user-friendly kinetic-fitting program 'kinmodel'.

Conflicts of Interest

The authors declare no conflicts of interest.

Data Availability Statement

The data that support the findings of this study are available in the Supporting Information of this article.

References

1. A. S. Y. Wong and W. T. S. Huck, "Grip on Complexity in Chemical Reaction Networks," *Beilstein Journal of Organic Chemistry* 13 (2017): 1486–1497, https://doi.org/10.3762/bjoc.13.147.

2. N. A. Yewdall, A. F. Mason, and J. C. M. van Hest, "The Hallmarks of Living Systems: Towards Creating Artificial Cells," *Interface Focus* 8 (2018): 20180023, https://doi.org/10.1098/rsfs.2018.0023.

3. K. B. Muchowska, S. J. Varma, and J. Moran, "Synthesis and Breakdown of Universal Metabolic Precursors Promoted by Iron," *Nature* 569 (2019): 104–107, https://doi.org/10.1038/s41586-019-1151-1.

4. K. B. Muchowska, S. J. Varma, and J. Moran, "Nonenzymatic Metabolic Reactions and Life's Origins," *Chemical Reviews* 120 (2020): 7708–7744, https://doi.org/10.1021/acs.chemrev.0c00191.

5. P. Adamski, M. Eleveld, A. Sood, et al., "From Self-Replication to Replicator Systems en Route to De Novo Life," *Nature Reviews Chemistry* 4 (2020): 386–403, https://doi.org/10.1038/s41570-020-0196-x.

6. P. L. Urban, "Compartmentalised Chemistry: From Studies on the Origin of Life to Engineered Biochemical Systems," *New Journal of Chemistry* 38 (2014): 5135–5141, https://doi.org/10.1039/C4NJ00894D.

7. C. D. Keating, "Aqueous Phase Separation as a Possible Route to Compartmentalization of Biological Molecules," *Accounts of Chemical Research* 45 (2012): 2114–2124, https://doi.org/10.1021/ar200294y.

8. L. Gabrielli, L. Goldin, S. Chandrabhas, A. Dalla Valle, and L. J. Prins, "Chemical Information Processing by a Responsive Chemical System," *Journal of the American Chemical Society* 146 (2024): 2080–2088, https://doi.org/10.1021/jacs.3c11414.

9. S. Ghosh, M. G. Baltussen, A. C. Knox, et al., "A Recursive Enzymatic Competition Network Capable of Multitask Molecular Information Processing," *Nature Chemistry* 18 (2026): 302–308, https://doi.org/10.1038/s41557-025-01981-y.

10. D. Kroiss, G. Ashkenasy, A. B. Braunschweig, T. Tuttle, and R. V. Ulijn, "Catalyst: Can Systems Chemistry Unravel the Mysteries of the Chemical Origins of Life?," *Chem* 5 (2019): 1917–1920, https://doi.org/10.1016/j.chempr.2019.05.003.

11. R. Edri, L. D. Williams, and M. Frenkel-Pinter, "From Catalysis of Evolution to Evolution of Catalysis," *Accounts of Chemical Research* 57 (2024): 3081–3092, https://doi.org/10.1021/acs.accounts.4c00196.

12. L. López-Maury, S. Marguerat, and J. Bähler, "Tuning Gene Expression to Changing Environments: From Rapid Responses to Evolutionary Adaptation," *Nature Reviews Genetics* 9 (2008): 583–593, https://doi.org/10.1038/nrg2398.

25704206, 2026, 6, Downloaded from https://chemistry-europe.onlinelibrary.wiley.com/doi/10.1002/syst.70059 by Chung-Ang University, Wiley Online Library on [20/11/2026]. See the Terms and Conditions (https://onlinelibrary.wiley.com/terms-and-conditions) on Wiley Online Library for rules of use; OA articles are governed by the applicable Creative Commons License

13. V. M. Weake and J. L. Workman, "Inducible Gene Expression: Diverse Regulatory Mechanisms," *Nature Reviews Genetics* 11 (2010): 426–437, https://doi.org/10.1038/nrg2781.

14. S. Bahrami and F. Drabløs, "Gene Regulation in the Immediate-Early Response Process," *Advances in Biological Regulation* 62 (2016): 37–49, https://doi.org/10.1016/j.jbior.2016.05.001.

15. W. E. Robinson, E. Daines, P. van Duppen, T. de Jong, and W. T. S. Huck, "Environmental Conditions Drive Self-Organization of Reaction Pathways in a Prebiotic Reaction Network," *Nature Chemistry* 14 (2022): 623–631, https://doi.org/10.1038/s41557-022-00956-7.

16. F. Jacob and J. Monod, "Genetic Regulatory Mechanisms in the Synthesis of Proteins," *Journal of Molecular Biology* 3 (1961): 318–356, https://doi.org/10.1016/S0022-2836(61)80072-7.

17. L. Shi and B. P. Tu, "Acetyl-CoA and the Regulation of Metabolism: Mechanisms and Consequences," *Current Opinion in Cell Biology* 33 (2015): 125–131, https://doi.org/10.1016/j.ceb.2015.02.003.

18. A. J. Lopatkin, S. C. Bening, A. L. Manson, et al., "Clinically Relevant Mutations in Core Metabolic Genes Confer Antibiotic Resistance," *Science* 371 (2021): eaba0862, https://doi.org/10.1126/science.aba0862.

19. A. Pal, D. Ghosh, P. Thakur, et al., "Clinically Relevant Mutations in Regulatory Regions of Metabolic Genes Facilitate Early Adaptation to Ciprofloxacin in Escherichia coli," *Nucleic Acids Research* 52 (2024): 10385–10399, https://doi.org/10.1093/nar/gkae719.

20. C. Josephides and P. S. Swain, "Predicting Metabolic Adaptation From Networks of Mutational Paths," *Nature Communications* 8 (2017): 685, https://doi.org/10.1038/s41467-017-00828-6.

21. T. Pols, H. R. Sikkema, B. F. Gaastra, et al., "A Synthetic Metabolic Network for Physicochemical Homeostasis," *Nature Communications* 10 (2019): 4239, https://doi.org/10.1038/s41467-019-12287-2.

22. H. W. H. van Roekel, B. J. H. M. Rosier, L. H. H. Meijer, et al., "Programmable Chemical Reaction Networks: Emulating Regulatory Functions in Living Cells Using a Bottom-up Approach," *Chemical Society Reviews* 44 (2015): 7465–7483.

23. M. J. Eleveld, J. Wu, K. Liu, et al., "Departure From Randomness: Evolution of Self-Replicators That Can Self-Sort Through Steric Zipper Formation," *Chem* 11 (2025): 102374, https://doi.org/10.1016/j.chempr.2024.11.012.

24. M. Steiner and M. Reiher, "Autonomous Reaction Network Exploration in Homogeneous and Heterogeneous Catalysis," *Topics in Catalysis* 65 (2022): 6–39, https://doi.org/10.1007/s11244-021-01543-9.

25. S. Yang, Y. Geiger, M. Geerts, M. J. Eleveld, A. Kiani, and S. Otto, "Enantioselective Self-Replicators," *Journal of the American Chemical Society* 145 (2023): 16889–16898, https://doi.org/10.1021/jacs.3c05472.

26. S. N. Semenov, L. J. Kraft, A. Ainla, et al., "Autocatalytic, Bistable, Oscillatory Networks of Biologically Relevant Organic Reactions," *Nature* 537 (2016): 656–660, https://doi.org/10.1038/nature19776.

27. M. ter Harmsel, O. R. Maguire, S. A. Runikhina, A. S. Y. Wong, W. T. S. Huck, and S. R. Harutyunyan, "A Catalytically Active Oscillator Made From Small Organic Molecules," *Nature* 621 (2023): 87–93.

28. Z. Zhang, M. G. Howlett, E. Silvester, P. Kukura, and S. P. Fletcher, "A Chemical Reaction Network Drives Complex Population Dynamics in Oscillating Self-Reproducing Vesicles," *Journal of the American Chemical Society* 146 (2024): 18262–18269, https://doi.org/10.1021/jacs.4c00860.

29. S. M. Morrow, I. Colomer, and S. P. Fletcher, "A Chemically Fuelled Self-Replicator," *Nature Communications* 10 (2019): 1011, https://doi.org/10.1038/s41467-019-08885-9.

30. A. Sood, P. K. Mandal, J. Ottelé, et al., "Simultaneous Formation of a Foldamer and a Self-Replicator by out-of-Equilibrium Dynamic Covalent Chemistry," *Journal of the American Chemical Society* 146 (2024): 33386–33394, https://doi.org/10.1021/jacs.4c09111.

31. M. J. Eleveld, Y. Geiger, J. Wu, A. Kiani, G. Schaeffer, and S. Otto, "Competitive Exclusion Among Self-Replicating Molecules Curtails the Tendency of Chemistry to Diversify," *Nature Chemistry* 17 (2025): 132–140, https://doi.org/10.1038/s41557-024-01664-0.

32. E. A. J. Post and S. P. Fletcher, "Dissipative Self-Assembly, Competition and Inhibition in a Self-Reproducing Protocell Model," *Chemical Science* 11 (2020): 9434–9442, https://doi.org/10.1039/D0SC02768E.

33. A. Venugopal, S. Ghosh, A. Calò, G. M. Tuveri, G. Battaglia, and M. Kumar, "Enzyme Controlled Transient Phospholipid Vesicles for Regulated Cargo Release," *Angewandte Chemie International Edition* 64 (2025): e202500824, https://doi.org/10.1002/anie.202500824.

34. C. Donau, F. Späth, M. Sosson, et al., "Active Coacervate Droplets as a Model for Membraneless Organelles and Protocells," *Nature Communications* 11 (2020): 5167, https://doi.org/10.1038/s41467-020-18815-9.

35. R. W. Lewis, B. Klemm, M. Macchione, and R. Eelkema, "Fuel-Driven Macromolecular Coacervation in Complex Coacervate Core Micelles," *Chemical Science* 13 (2022): 4533–4544, https://doi.org/10.1039/D2SC00805J.

36. J. Chen, S. Körner, S. L. Craig, D. M. Rudkevich, and J. Rebek, "Amplification by Compartmentalization," *Nature* 415 (2002): 385–386, https://doi.org/10.1038/415385b.

37. M. M. Hossain, J. L. Atkinson, and C. S. Hartley, "Dissipative Assembly of Macrocycles Comprising Multiple Transient Bonds," *Angewandte Chemie International Edition* 59 (2020): 13807–13813, https://doi.org/10.1002/anie.202001523.

38. C. M. E. Kriebisch, A. M. Bergmann, and J. Boekhoven, "Fuel-Driven Dynamic Combinatorial Libraries," *Journal of the American Chemical Society* 143 (2021): 7719–7725, https://doi.org/10.1021/jacs.1c01616.

39. C. M. E. Kriebisch, L. Burger, O. Zozulia, et al., "Template-Based Copying in Chemically Fuelled Dynamic Combinatorial Libraries," *Nature Chemistry* 16 (2024): 1240–1249, https://doi.org/10.1038/s41557-024-01570-5.

40. M. Valentini, G. Ercolani, and S. Di Stefano, "How Activated Carboxylic Acids can Drive Dissipative Systems," *ChemSystemsChem* 7 (2025): e00021, https://doi.org/10.1002/syst.202500021.

41. I. Aprahamian and S. M. Goldup, "Non-Equilibrium Steady States in Catalysis, Molecular Motors, and Supramolecular Materials: Why Networks and Language Matter," *Journal of the American Chemical Society* 145 (2023): 14169–14183, https://doi.org/10.1021/jacs.2c12665.

42. Y. Zhao, P. Zhao, J. Zhang, et al., "Light-Controlled Chemical Reaction Pathways in Disulfide-Based Nonequilibrium Systems," *CCS Chemistry* 6 (2024): 1571–1580, https://doi.org/10.31635/ccschem.023.202303331.

43. Y. Zhao, B. Li, X. Fu, et al., "Autocatalytic Reaction Networks: A Pathway to Spatial Temporal Mastery in Dynamic Materials," *Angewandte Chemie International Edition* 64 (2025): e202415582, https://doi.org/10.1002/anie.202415582.

44. Y. Zhao, Y. Zhao, P. Zhao, et al., "A Closed-Loop Chemical Reaction Network for Autonomous, Dual-Window Temporal Programming from a Single Fuel Pulse," *Angewandte Chemie International Edition* 65 (2026): e202524255.

45. P. Zhao, Y. Zhao, Y. Lu, et al., "Non-Equilibrium Dissipative Assembly With Switchable Biological Functions," *Angewandte Chemie International Edition* 63 (2024): e202409169, https://doi.org/10.1002/anie.202409169.

46. M. G. Baltussen, T. J. de Jong, Q. Duez, W. E. Robinson, and W. T. S. Huck, "Chemical Reservoir Computation in a Self-Organizing Reaction Network," *Nature* 631 (2024): 549–555, https://doi.org/10.1038/s41586-024-07567-x.

47. B. J. Cafferty, A. S. Y. Wong, S. N. Semenov, et al., "Robustness, Entrainment, and Hybridization in Dissipative Molecular Networks, and the Origin of Life," *Journal of the American Chemical Society* 141 (2019): 8289–8295, https://doi.org/10.1021/jacs.9b02554.

48. D. Del Giudice, M. Valentini, G. Melchiorre, E. Spatola, and S. Di Stefano, "Dissipative Dynamic Covalent Chemistry (DDCvC) Based on

25704206, 2026, 6, Downloaded from https://chemistry-europe.onlinelibrary.wiley.com/doi/10.1002/syst.70059 by Chung-Ang University, Wiley Online Library on [20/11/2026]. See the Terms and Conditions (https://onlinelibrary.wiley.com/terms-and-conditions) on Wiley Online Library for rules of use; OA articles are governed by the applicable Creative Commons License

the Transimination Reaction," *Chemistry – A European Journal* 28 (2022): e202200685..

49. P. van Duppen, E. Daines, W. E. Robinson, and W. T. S. Huck, "Dynamic Environmental Conditions Affect the Composition of a Model Prebiotic Reaction Network," *Journal of the American Chemical Society* 145 (2023): 7559–7568.

50. G. Melchiorre, L. Visieri, M. Valentini, et al., "Imine-Based Transient Supramolecular Polymers," *Journal of the American Chemical Society* 147 (2025): 11327–11335, https://doi.org/10.1021/jacs.5c00274.

51. Y. Lim, G. Park, H. An, et al., "Metabolism-Inspired Chemical Reaction Networks for Chemically Driven Dissipative Oligoesterification," *Angewandte Chemie International Edition* 64 (2025): e202425407, https://doi.org/10.1002/anie.202425407.

52. I. M. Jayalath, H. Wang, G. Mantel, L. S. Kariyawasam, and C. S. Hartley, "Chemically Fueled Transient Geometry Changes in Diphenic Acids," *Organic Letters* 22 (2020): 7567–7571, https://doi.org/10.1021/acs.orglett.0c02757.

53. M. M. Hossain, I. M. Jayalath, R. Baral, and C. S. Hartley, "Carbodiimide-Induced Formation of Transient Polyether Cages**," *ChemSystemsChem* 4 (2022): e202200016, https://doi.org/10.1002/syst.202200016.

54. L. S. Kariyawasam and C. S. Hartley, "Dissipative Assembly of Aqueous Carboxylic Acid Anhydrides Fueled by Carbodiimides," *Journal of the American Chemical Society* 139 (2017): 11949–11955, https://doi.org/10.1021/jacs.7b06099.

55. X. Chen, H. Soria-Carrera, O. Zozulia, and J. Boekhoven, "Suppressing Catalyst Poisoning in the Carbodiimide-Fueled Reaction Cycle," *Chemical Science* 14 (2023): 12653–12660, https://doi.org/10.1039/D3SC04281B.

56. I. M. Jayalath, M. M. Gerken, G. Mantel, and C. S. Hartley, "Substituent Effects on Transient, Carbodiimide-Induced Geometry Changes in Diphenic Acids," *Journal of Organic Chemistry* 86 (2021): 12024–12033, https://doi.org/10.1021/acs.joc.1c01385.

57. L. S. Kariyawasam, J. C. Kron, R. Jiang, A. J. Sommer, and C. S. Hartley, "Structure–Property Effects in the Generation of Transient Aqueous Benzoic Acid Anhydrides by Carbodiimide Fuels," *Journal of Organic Chemistry* 85 (2020): 682–690, https://doi.org/10.1021/acs.joc.9b02746.

58. K. A. Johnson, Z. B. Simpson, and T. Blom, "FitSpace Explorer: An Algorithm to Evaluate Multidimensional Parameter Space in Fitting Kinetic Data," *Analytical Biochemistry* 387 (2009): 30–41, https://doi.org/10.1016/j.ab.2008.12.025.

59. M.-Y. Kim and I.-H. Um, "Kinetic Study on Aminolysis of O-2-Pyridyl Thionobenzoate in Acetonitrile: Effect of Changing Electrophilic Center From C-O to C-S on Reactivity and Reaction Mechanism," *Bulletin of the Korean Chemical Society* 37 (2016): 1401–1405, https://doi.org/10.1002/bkcs.10875.

60. S. Y. Pyun, K. C. Paik, M. S. Han, and B. R. Cho, "Reactions of 2,4-Dinitrophenyl 5-Substituted-2-Thiophenecarboxylates With $R_2NH/R_2NH_2^+$ in 20 Mol % DMSO(aq). Effects of 5-Thienyl Substituent and Leaving Group on the Reaction Mechanism," *Bulletin of the Korean Chemical Society* 40 (2019): 983–990, https://doi.org/10.1002/bkcs.11857.

61. E.-J. Yang, M.-Y. Kim, and I.-H. Um, "Kinetic Study on Quinuclidinolysis of O -4-Nitrophenyl X-Substituted Thionobenzoates and O -3,4-Dinitrophenyl Thionobenzoate: Effect of Amine Nature on Reactivity and Reaction Mechanism," *Bulletin of the Korean Chemical Society* 36 (2015): 1551–1556, https://doi.org/10.1002/bkcs.10293.

62. E. W. Della, "Conformational Analysis. Trifluoromethyl Group," *Journal of the American Chemical Society* 89 (1967): 5221–5224, https://doi.org/10.1021/ja00996a024.

63. H. J. Schneider and V. Hoppen, "Carbon-13 Nuclear Magnetic Resonance Substituent-Induced Shieldings and Conformational Equilibriums in Cyclohexanes," *Journal of Organic Chemistry* 43 (1978): 3866–3873, https://doi.org/10.1021/jo00414a017.

64. K. Yamada and T. Inokuma, "Evaluation of Quantum Chemistry Calculation Methods for Conformational Analysis of Organic Molecules Using A-Value Estimation as a Benchmark Test," *RSC Advances* 13 (2023): 35904–35910, https://doi.org/10.1039/D3RA06783A.

65. S. M. Blau, H. D. Patel, E. W. C. Spotte-Smith, X. Xie, S. Dwaraknath, and K. A. Persson, "A Chemically Consistent Graph Architecture for Massive Reaction Networks Applied to Solid-Electrolyte Interphase Formation," *Chemical Science* 12 (2021): 4931–4939, https://doi.org/10.1039/D0SC05647B.

66. J. P. Unsleber, "Accelerating Reaction Network Explorations With Automated Reaction Template Extraction and Application," *Journal of Chemical Information and Modeling* 63 (2023): 3392–3403, https://doi.org/10.1021/acs.jcim.3c00102.

67. V. Nanda, J. Siess, B. P. Jagilinki, et al., "On the Emergence of Metabolism: The Evolution of Proteins That Powered Life," *Philosophical Transactions of the Royal Society B: Biological Sciences* 380 (2025): 20240090, https://doi.org/10.1098/rstb.2024.0090.

68. K. Ruiz-Mirazo, C. Briones, and A. de la Escosura, "Prebiotic Systems Chemistry: New Perspectives for the Origins of Life," *Chemical Reviews* 114 (2014): 285–366, https://doi.org/10.1021/cr2004844.

Supporting Information

Additional supporting information can be found online in the Supporting Information section.

Supporting File: syst70059-sup-0001-SuppMat.zip Supporting File: syst70059-sup-0002-SuppMat.pdf Supporting File: syst70059-sup-0003-Movie1.mp4 Supporting File: syst70059-sup-0004-Movie2.mp4 Supporting File: syst70059-sup-0005-Movie3.mp4

25704206, 2026, 6, Downloaded from https://chemistry-europe.onlinelibrary.wiley.com/doi/10.1002/syst.70059 by Chung-Ang University, Wiley Online Library on [20/11/2026]. See the Terms and Conditions (https://onlinelibrary.wiley.com/terms-and-conditions) on Wiley Online Library for rules of use; OA articles are governed by the applicable Creative Commons License